

A Modal Analysis-Based Cloud-Shaped Flexible Two-Element CPW-Fed Antenna For 5G Wireless Applications

Deepthi Mariam John¹, Tanweer Ali^{1,*}, Shweta Vincent², Sameena Pathan³, Kirti Panwar Bhati⁴, Manish Varun Yadav⁵

¹Department of Electronics and Communication Engineering, Manipal Institute of Technology, Manipal, Academy of Higher Education, Manipal 576104, India

²Department of Mechatronics, Manipal Institute of Technology, Manipal, Academy of Higher Education, Manipal 576104, India

³Department of Information and Communication Technology, Manipal Institute of Technology, Manipal, Academy of Higher Education, Manipal 576104, India

⁴School of Electronics, Devi Ahilya University, Indore 452001, Madhya Pradesh, India

⁵Department of Aeronautical & Automobile Engineering, Manipal Institute of Technology, Manipal, Academy of Higher Education, Manipal 576104, India

*Author to whom correspondence should be addressed:
E-mail: tanweer.ali@manipal.edu

(Received September 27, 2024; Revised April 17, 2025; Accepted April 24, 2025)

Abstract: This article presents a highly flexible coplanar waveguide (CPW) fed MIMO antenna that consists of a cloud-shaped modified circular radiator, and a connected self-isolating decoupling structure. The antenna has an overall size of $0.468\lambda \times 0.819\lambda \times 0.0013\lambda$ (λ is computed at 3.9 GHz) with a bandwidth of 3.90-5.13 GHz. Characteristic mode analysis (CMA) is investigated to understand the proposed antenna's physical nature. The antenna offers a peak gain of 4.1 dBi at the resonant frequency (4.6 GHz) and an average efficiency of 89% throughout the operating range. MIMO diversity metrics also show favorable results suitable for wireless applications.

Keywords: 5G; CMA; CPW; multiple-input-multiple-output (MIMO)

1. Introduction

The substantial development of fifth-generation wireless technology paves the way for the development of several sectors including IoT, military, wearable technology, medical informatics, surveillance applications, and so on¹⁻⁵. Among them, wearable technology is on trend due to its feasibility in integrating several smart devices. Therefore, wearable antennas with high flexibility, compactness, and good performance are in high demand. MIMO systems can expand the channel's transmission capacity and therefore have gained reasonable recognition over the past years⁶⁻⁹. However, mutual coupling among the interelement of the MIMO antenna is a critical problem that further declines the antenna performance.

The literature contributes various methods for decrementing the mutual coupling like a defective ground plane¹⁰⁻¹⁴, orthogonal orientation¹⁵⁻¹⁸, metamaterials¹⁹⁻²⁰, neutralization line²¹⁻²⁵, self-isolating structures²⁶⁻²⁷, parasitic elements²⁸, Jerusalem cross absorbers²⁹ and so on. A two-element antenna with a via less decoupling

methodology is proposed in¹¹. The stubs attached to the feedline with a slotted ground plane offer isolation of 16 dB. A quad-element antenna fed by a coplanar waveguide (CPW) is elaborated in¹⁵ for 5G mid-band. The antenna has improved bandwidth, gain, and diversity metrics with an isolation of 18 dB but occupies a large antenna volume. A conformal MIMO is presented in¹⁶ for 5G and IoT applications. The antenna offers a wider bandwidth with an isolation of 17.5 dB, but the gain is meager. A two-element antenna incorporating meta-inspired decoupling methodology is proposed in¹⁹. The orthogonal orientation of the antenna contributes to 30 dB isolation. Nevertheless, the antenna volume is comparatively high, and the gain is very low. A four-element antenna with octagonal rings in the radiator is proposed in²⁶ with good gain and diversity metrics, but the antenna is bulky in size. From the literature, it is clear that a flexible antenna design that satisfies all the above-mentioned antenna characteristics with a compact size is a very challenging task.

The paper proposes a flexible dual-element antenna with a self-isolating decoupling structure for 5G mid-band. The

antenna contributes 4.1 dBi gain and 89% efficiency at the resonance and has 3.9-5.13 GHz bandwidth. CMA provides clear information about the antenna radiation characteristics as well as the significant modes. MIMO diversity parameters are estimated for checking the antenna feasibility in a real-time scenario. Section 2 of the article covers antenna design, followed by Section 3 on CMA, Section 4 on Results and Discussion, and Section 5 on Conclusion.

2. Antenna Design

A cloud-shaped modified radiator with a CPW ground has been horizontally duplicated to form a highly isolated two-element antenna (antenna1) as visualized in Figure 1. The two elements are placed at a minimal distance of 3mm which is very much less than one-fourth of the wavelength. As seen from the Figure, it is evident that antenna1 has a self-isolating structure that covers 3.92-5.15 GHz bandwidth with -20 dB isolation over the bandwidth as seen from Figure 2. Further, to connect the ground plane, the antenna2 (proposed) is integrated with two rectangular stubs as given in Figure 1.

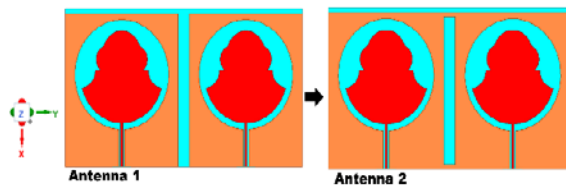


Fig. 1: Proposed antenna evolution without and with connected ground

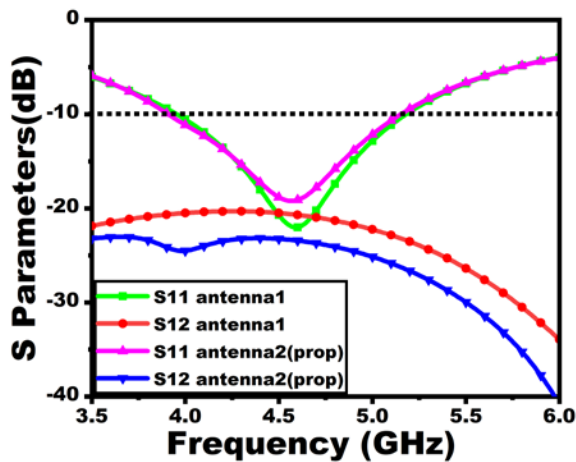


Fig. 2: S-parameter of antenna1 and antenna2 (proposed)

Integrating the stubs in the second stage creates a deviation in the current path, which is opposite in phase to that of the coupling current. It could be further investigated using the vector current distribution of the antenna analyzed at the resonant frequency as portrayed in Figure 3. It is evident from the current distribution plot that when the first port is excited, there is a minimal influence of the current in the

second element due to the effect of the rectangular stubs that create an opposite phase current which contributes to enhanced inter-element isolation of 23 dB over the functional band of operation between 3.9-5.13 GHz. Figure 4 gives the values of each antenna parameter.

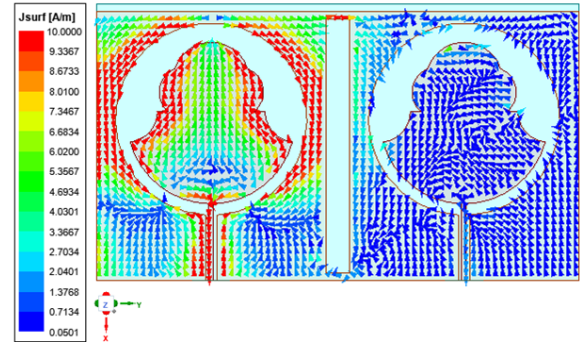


Fig. 3: Vector current distribution of the suggested antenna at 4.6 GHz

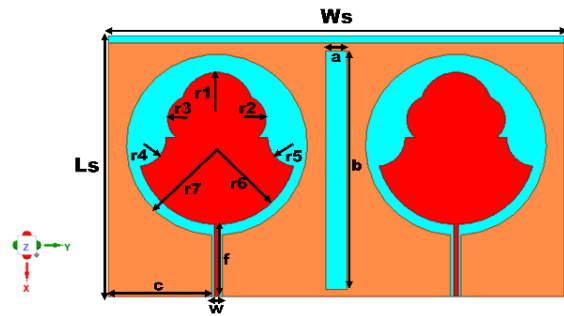


Fig. 4: Dimension of the antenna (in mm): Ws=63, Ls=36, a=3, b=33, c=14, f=10, w=0.6, r1=5, r2=3.3, r3=3.3, r4=4, r5=4, r6=11 and r7=12

3. Characteristic Mode Analysis

The theory of CMA has proven to be a very helpful aid in investigating the physical nature of any conducting structure. According to CMA, any arbitrary conducting structure can be taken as the union of modal functions³⁰⁻³². The total current J is the combination of the currents associated with n th modes for a structure as given in equation (1)³⁰.

$$J = \sum_n \frac{\iiint (J_n E^i) d\tau}{1 + j\lambda_n} J_n \quad (1)$$

where J_n represents the n th mode current and λ_n is the eigenvalue. A mode resonates when the eigenvalue is zero. The antenna's characteristic angle (CA) and modal significance (MS) provide information about the antenna radiation. MS accounts for normalized amplitudes and CA accounts for the phase difference between field and current as given in equations (2-3). Each mode has a maximum MS value of 1. The more each mode tends to be closer to 1, the more likely the corresponding modes contribute to antenna radiation.

$$MS = \left| \frac{1}{1+j\lambda_n} \right| \quad (2)$$

$$CA = 180^\circ - \tan^{-1}\lambda_n \quad (3)$$

Figure 5 depicts the CMA for the first five fundamental modes. All modes possess significance based on the MS graphs. Nevertheless, since the MS values of modes 1 and 2 achieve resonance ($MS = 1$) close to the antenna's resonance frequency, they contribute substantially to the resonance of the antenna. This could be justified while investigating the CA and eigenvalue plots given in Figure 5. No modes in the MS plot have a superposition that validates satisfactory impedance matching. Table 1 lists the CMA parameters and their characteristics with respect to each CM modes. All the modes except mode 3 are inductive in nature with eigen value greater than zero and CA less than 1800. The corresponding mode resonates when the eigen value is unity and CA of the corresponding mode is 1800. However, it is inferred that all the modes are significant with a value greater than 0.707 at the resonant frequency of the antenna with modes 1 and 2 providing utmost significance. The vector current distribution and far-field patterns of the CM modes are displayed in Figure 6 and Figure 7 respectively. The suggested antenna provides stable radiation characteristics for all the CM modes. The first five fundamental modes are given as M1-M5 for better understanding.

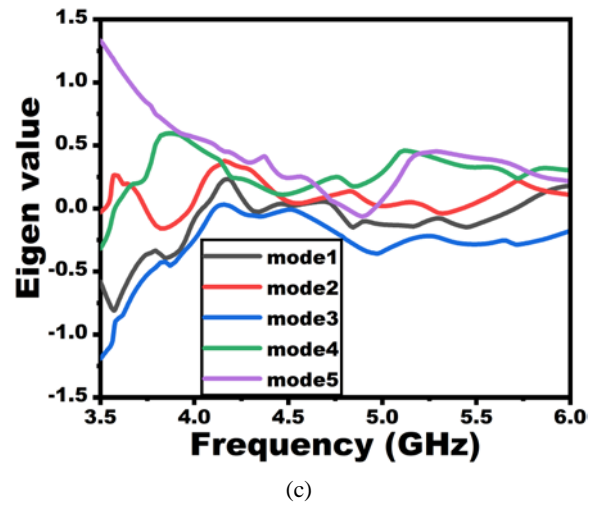
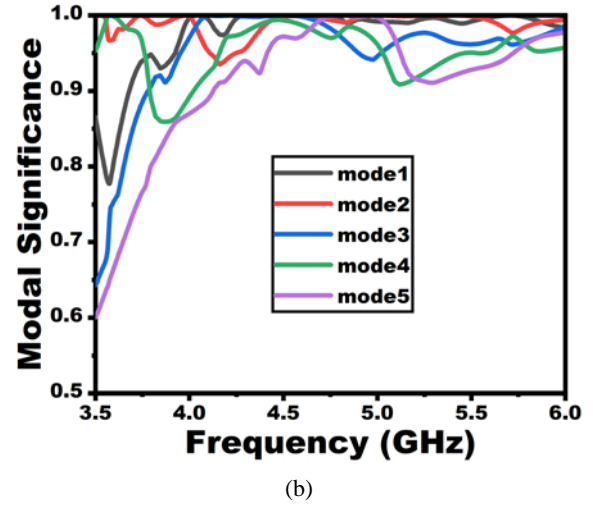
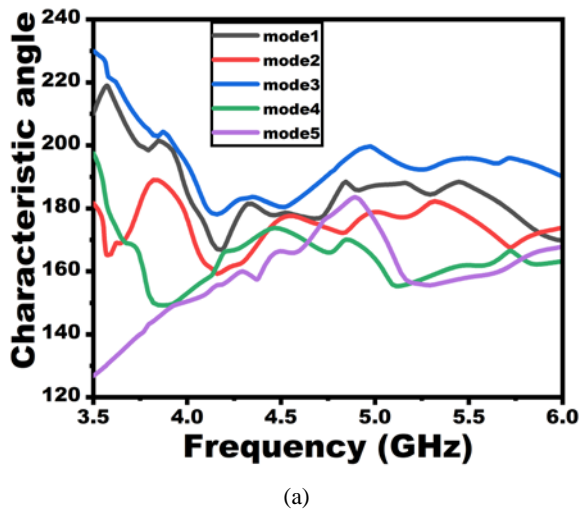


Fig. 5: CMA (a) CA (b) MS, and (c) Eigenvalue

Table 1: CMA parameters and its characteristics

Freq (GHz)	Mode s	Eigen value	MS	CA	Inference
4.6	M1	0.041	0.999	177.63	Inductive
	M2	0.051	0.998	177.08	Inductive
	M3	-0.058	0.998	183.37	Capacitive
	M4	0.161	0.987	170.81	Inductive
	M5	0.236	0.973	166.68	Inductive

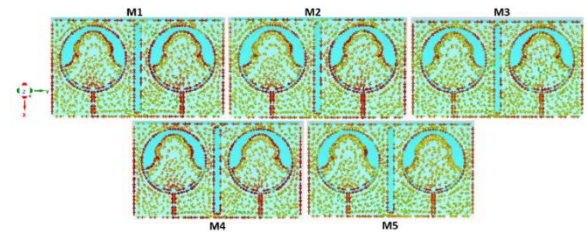


Fig. 6: Current distribution of all CM modes

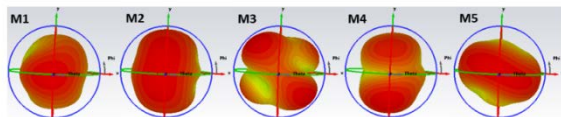


Fig. 7: Field patterns of all CM modes

4. Results and Discussion

4.1. Scattering Parameters

The design is executed using the HFSS simulator and has 3.9-5.13 GHz bandwidth with 23 dB isolation throughout the frequency of operation. The S-parameters are compared with the CST MWS EM simulator and the results are in line as shown in Figure 8.

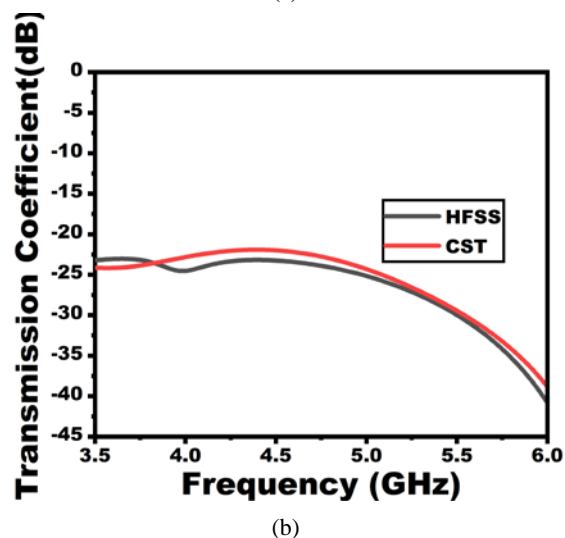
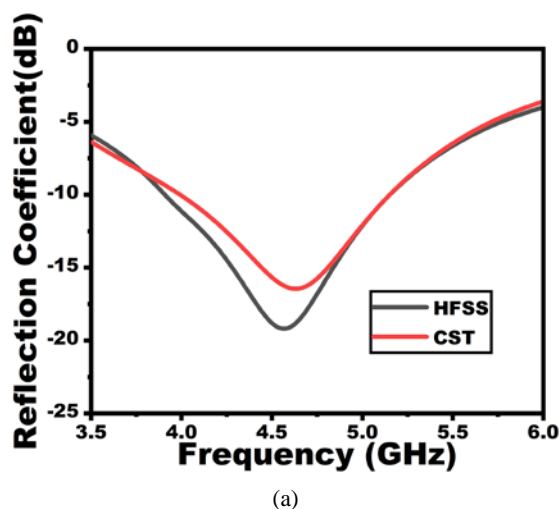


Fig. 8: Antenna S-Parameters

4.2. Current distribution

Figure 9 provides information about the antenna's magnitude current concentration. It can be observed that there is very little current concentration at the adjusting element, indicating improved isolation and also the current accumulates along the feedline, ground, and edges of the excited element's radiator.

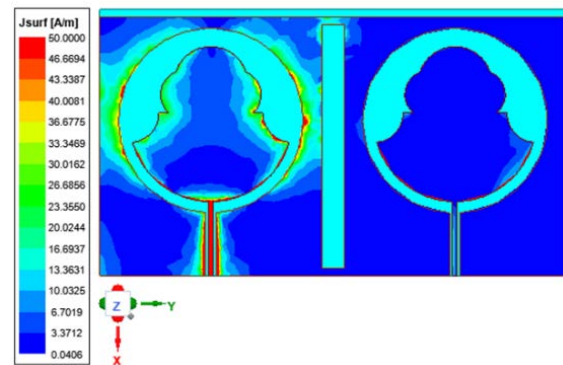


Fig. 9: Current distribution at 4.6 GHz

4.3. Radiation Pattern

The radiation properties at 4.6 GHz for the presented antenna are displayed in Figure 10. As seen in the Figure, an omnidirectional and bidirectional pattern in the H plane (YZ, $\phi = 90^\circ$) in the E plane (XZ, $\phi = 0^\circ$) respectively is exhibited by the proposed antenna.

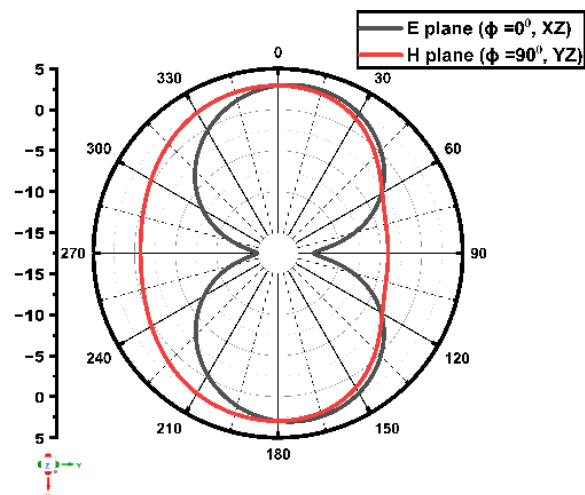


Fig. 10: Radiation pattern at 4.6 GHz

Figure 11 shows the max gain and radiation efficiency v/s frequency plot. The antenna exhibits a maximum gain and efficiency of 4.1 dBi and 89% as seen in the Figure

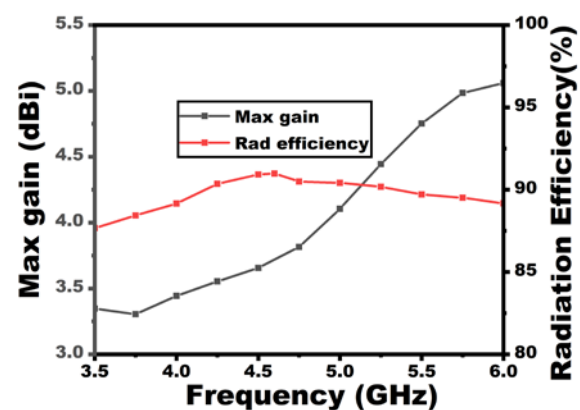


Fig. 11: Maximum gain and radiation efficiency

4.4. MIMO diversity parameters

Diversity measurements are examined to comprehend the antenna's potential for use in real-time MIMO applications. The correlation between each element is provided by the envelope correlation coefficient (ECC). Diversity gain (DG) has to remain high for quality communication and it is estimated using the ECC as per equation 4³³). An essential parameter for accurately expressing bandwidth and antenna efficiency is the total active reflection coefficient or TARC³⁴). The lossless message transmission in a communication channel is estimated by channel capacity loss (CCL)³⁵). The ratio of received power at the diversity to isotropic antennas is called the mean effective gain. Multiplexing efficiency evaluates the correlation of multiple elements³⁶⁻³⁷). The diversity metrics are calculated using equations (4-9).

$$ECC = \frac{|S_{ii}^* S_{ij} + S_{ji}^* S_{jj}|^2}{(1 - |S_{ii}|^2 - |S_{jj}|^2)(1 - |S_{jj}|^2 - |S_{ii}|^2)} \quad (4)$$

$$DG = 10\sqrt{1 - ECC^2} \quad (5)$$

$$TARC = N^{-0.5} \sqrt{\sum_{i=1}^N |\sum_{k=1}^N S_{ik} e^{j\theta_{k-1}}|^2} \quad (6)$$

$$MEG_i = 0.5\eta_{i,rad} = 0.5(1 - \sum_{j=1}^p |S_{ij}|) \quad (7)$$

where

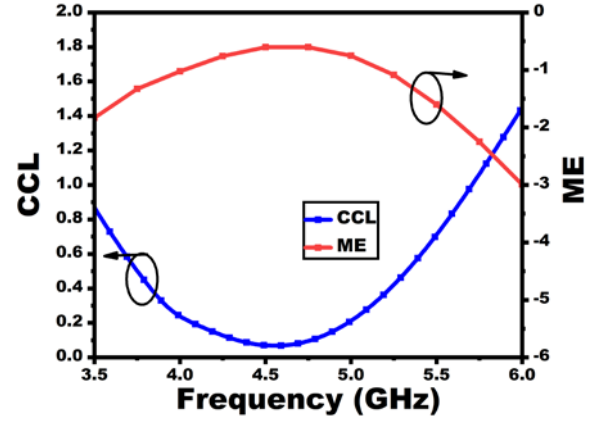
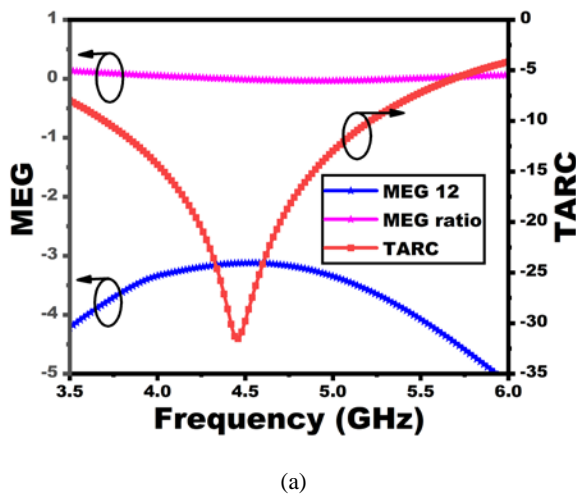
$$\alpha_{ii} = 1 - n = 1 - NSin * S_{ni} \text{ for } i, j = 1, 2, 3, 4, \dots$$

$$\alpha_{ij} = 1 - n = 1 - NSin * S_{nj} \text{ for } i, j = 1, 2, 3, 4, \dots$$

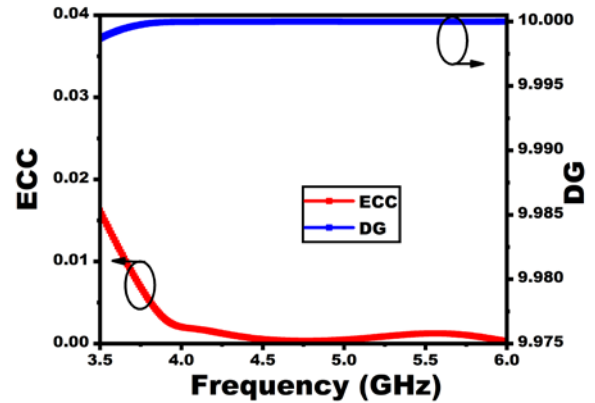
$$CCL = -\log_2 \det \alpha^R \quad (8)$$

$$ME = \sqrt{\eta_i \eta_j (1 - |\rho_{ij}|^2)} \quad (9)$$

Figure 12 shows the antenna's diversity metrics whose values are given in Table 3.



(b)



(c)

Fig. 12: MIMO diversity metrics (a) MEG and TARC (b) CCL and ME, and (c) ECC and DG

4.5. Comparative Analysis

Tables 2 and 3 compare the antenna with previously published works. The tables demonstrate that the suggested antenna performs appropriately with its bandwidth, MIMO diversity metrics, gain, and improved isolation.

Table 2: Proposed antenna comparison with existing works

Ref	Dimension (mm ³)/λ ³	Port	BW GHz	Gain dBi	Decoupling mechanism
¹¹⁾	32×40×1 mm ³ / 0.73×0.55×0.018λ ³	2	5.32 - 5.64	-	Stubs attached to feedline and slotted ground
¹⁵⁾	106.6×106.6×0.8 mm ³ / 1.41×1.41×0.01λ ³	4	1.95 -6.7	7	Trapezoidal slots in the ground plane
¹⁶⁾	110×116×1 mm ³ / 0.88×0.93×0.008λ ³	4	2.22 - 3.85	0.56	Stubs extended from the ground plane

¹⁹⁾	100×60×1 mm ³ / 0.8×0.48×0.008λ ³	2	1.34 - 6.34	3	Meta- inspired decoupling structure
²⁶⁾	70×145×0.2 mm ³ / 0.55×1.41×0.0015 λ ³	4	2.37 - 5.85	4	Octagonal rings with radiator
Pro p	36×63×0.1 mm ³ / 0.468×0.819×0.001 3λ ³	2	3.9- 5.13	4.1	Self- isolating decoupling structure

λ-computed at the lower frequency

Table 3: Comparison of MIMO diversity and isolation

Ref	ECC	DG	MEG	TA RC	CC L	ME	I*
¹¹⁾	<0.15	9.7	-	-	-	-	16
¹⁵⁾	<0.004	9.99	-	-	-	-	18
¹⁶⁾	<0.2	-	-	-	< 0.2	-	30
¹⁹⁾	<0.04	9	-	-	-	-	10
²⁶⁾	<0.05	9.8	-	-	-	-	17
Prop	<0.0025	9.99	<-3dB	<-10	<0.3 2	<- 0.5	23

I*-isolation

5. Conclusion

This paper communicates a flexible, efficient, highly isolated CPW-fed two-element antenna covering 3.90-5.13 GHz with a 4.1 dBi peak gain beneficial for the specific band. The antenna elements are kept at a minimal inter-element spacing and have an isolation of 23 dB. CMA of the antenna explains the eigenvalue-based parameters and gives information about the antenna radiation characteristics. MIMO diversity metrics give good results with ECC < 0.0025, CCL = 0.32 bps/Hz, DG > 9.99, ME < -0.5, MEG ~ -3 dB, and TARC < -10dB which is beneficial for 5G MIMO communications.

References

- 1) N.T.Atanasov, G.L. Atanasova, B. Angelova, M. Paunov, M. Gurmanova, and M. Kouzmanova, "Wearable antennas for sensor networks and iot applications: evaluation of sar and biological effects," *Sensors*, 22 (14) 5139 (2022). doi:10.3390/s22145139.
- 2) H.Yalduz, T.E. Tabaru, V.T. Kilic, and M. Turkmen, "Design and analysis of low profile and low sar full-textile uwb wearable antenna with metamaterial for wban applications," *AEU - International Journal of Electronics and Communications*, 126 153465 (2020). doi:10.1016/j.aeue.2020.153465.
- 3) M.A.Khan, W.T. Sethi, W.A. Malik, A. Jabbar, M.A. Khalid, A.M. Almuhlaifi, and M. Himdi, "A comprehensive analysis of low-profile dual band flexible omnidirectional wearable antenna for wban applications," *IEEE Access*, 12 45187–45201 (2024). doi:10.1109/ACCESS.2024.3380908.
- 4) E.Celenk, and N.T. Tokan, "All-textile on-body antenna for military applications," *Antennas Wirel. Propag. Lett.*, 21 (5) 1065–1069 (2022). doi:10.1109/LAWP.2022.3159301.
- 5) F.R.Kareem, A.A. Ibrahim, and M.A. Abdalla, "Triple-band monopole textile wearable antenna for iomt application," *IEEE Sensors J.*, 23 (19) 23377–23387 (2023). doi:10.1109/JSEN.2023.3305917.
- 6) C.Munusami, and R. Venkatesan, "A compact boat shaped dual-band mimo antenna with enhanced isolation for 5g/wlan application," *IEEE Access*, 12 11631–11641 (2024). doi:10.1109/ACCESS.2024.3356078.
- 7) J.Kulkarni, A.G. Alharbi, C.-Y.-D. Sim, I. Elfergani, J. Anguera, C. Zebiri, and J. Rodriguez, "Dual polarized, multiband four-port decagon shaped flexible mimo antenna for next generation wireless applications," *IEEE Access*, 10 128132–128150 (2022). doi:10.1109/ACCESS.2022.3227034.
- 8) P.Kumar, T. Ali, S. Pathan, N. Kumar Shetty, Y. Bommenahalli Huchegowda, and Y. Nanjappa, "Design and analysis of ultra-wideband four-port mimo antenna with dgs as decoupling structure for thz applications," *Results in Optics*, 13 100573 (2023). doi:10.1016/j.rio.2023.100573.
- 9) P.Sharma, R.N. Tiwari, P. Singh, and B.K. Kanaujia, "Dual-band trident shaped mimo antenna with novel ground plane for 5g applications," *AEU - International Journal of Electronics and Communications*, 155 154364 (2022). doi:10.1016/j.aeue.2022.154364.
- 10) A.K.Saurabh, and M.K. Meshram, "Compact sub - 6 GHz 5G - multiple - input - multiple - output antenna system with enhanced isolation," *Int J RF Microw Comput Aided Eng*, 30 (8) (2020). doi:10.1002/mmce.22246.
- 11) A.A.Ghannad, M. Khalily, P. Xiao, R. Tafazolli, and A.A. Kishk, "Enhanced matching and vialess decoupling of nearby patch antennas for mimo system," *Antennas Wirel. Propag. Lett.*, 18 (6) 1066–1070 (2019). doi:10.1109/LAWP.2019.2906308.
- 12) S.B.Kempanna, R.C. Biradar, P. Kumar, P. Kumar, S. Pathan, and T. Ali, "Characteristic-mode-analysis-based compact vase-shaped two-element uwb mimo antenna using a unique dgs for wireless communication," *JSAN*, 12 (3) 47 (2023). doi:10.3390/jsan12030047.
- 13) J.Kulkarni, C.-Y.-D. Sim, A. Desai, E. Holdengreber, R. Talware, V. Deshpande, and T.K. Nguyen, "A compact four port ground-coupled cpwg-fed mimo

- antenna for wireless applications,” *Arab J Sci Eng*, 47 (11) 14087–14103 (2022). doi:10.1007/s13369-022-06620-z.
- 14) I.S.Masoodi, I. Ishteyaq, and K. Muzaffar, “EXTRA compact two element sub 6 ghz mimo antenna for future 5g wireless applications,” *PIER Letters*, 102 37–45 (2022). doi:10.2528/PIERL21100303.
- 15) C.Du, and Y. Ren, “A cpw-fed wideband four-port mimo slot antenna with high isolation for sub-6g applications,” *Journal of Electromagnetic Waves and Applications*, 38 (4) 428–442 (2024). doi:10.1080/09205071.2024.2315578.
- 16) X.Zhou, T. Leng, K. Pan, M. Abdalla, K.S. Novoselov, and Z. Hu, “Conformal screen printed graphene 4×4 wideband mimo antenna on flexible substrate for 5g communication and iot applications,” *2D Mater.*, 8 (4) 045021 (2021). doi:10.1088/2053-1583/ac1959.
- 17) Md.M.Hasan, M.T. Islam, M. Samsuzzaman, M.H. Baharuddin, M.S. Soliman, A. Alzamil, I.I.M. Abu Sulayman, and Md.S. Islam, “Gain and isolation enhancement of a wideband mimo antenna using metasurface for 5g sub-6 ghz communication systems,” *Sci Rep*, 12 (1) 9433 (2022). doi:10.1038/s41598-022-13522-5.
- 18) M.A. Abdelghany, M. Fathy Abo Sree, A. Desai, and A. A. Ibrahim, “4-port octagonal shaped mimo antenna with low mutual coupling for uwb applications,” *Computer Modeling in Engineering & Sciences*, 136 (2) 1999–2015 (2023). doi:10.32604/cmes.2023.023643.
- 19) S.Roy, and U. Chakraborty, “Mutual coupling reduction in a multi-band mimo antenna using meta-inspired decoupling network,” *Wireless Pers Commun*, 114 (4) 3231–3246 (2020). doi:10.1007/s11277-020-07526-5.
- 20) D.Brizi, M. Conte, and A. Monorchio, “A performance-enhanced antenna for microwave biomedical applications by using metasurfaces,” *IEEE Trans. Antennas Propagat.*, 71 (4) 3314–3323 (2023). doi:10.1109/TAP.2023.3242414.
- 21) A.Kumar, P. Pattanayak, R.K. Verma, D. Sabat, and G. Prasad, “Two-element mimo antenna system for multiband millimeter-wave, 5g mobile communication, ka-band, and future 6g applications with sar analysis,” *AEU - International Journal of Electronics and Communications*, 171 154876 (2023). doi:10.1016/j.aeue.2023.154876.
- 22) M.Li, L. Jiang, and K.L. Yeung, “A general and systematic method to design neutralization lines for isolation enhancement in mimo antenna arrays,” *IEEE Trans. Veh. Technol.*, 69 (6) 6242–6253 (2020). doi:10.1109/TVT.2020.2984044.
- 23) W.A.Neamah, H.M.A. Sabbagh, and H. Al-Rizzo, “A compact two-element linearly and orthogonal circularly polarized mimo antenna system for 5g cellular and wlan/wi-fi 6e application,” *IEEE Access*, 11 96879–96891 (2023). doi:10.1109/ACCESS.2023.3312122.
- 24) R.N.Tiwari, P. Singh, B.K. Kanaujia, and K. Srivastava, “Neutralization technique based two and four port high isolation mimo antennas for uwb communication,” *AEU - International Journal of Electronics and Communications*, 110 152828 (2019). doi:10.1016/j.aeue.2019.152828.
- 25) A.K.Biswas, and U. Chakraborty, “Investigation on decoupling of wide band wearable multiple - input multiple - output antenna elements using microstrip neutralization line,” *Int J RF Microw Comput Aided Eng*, 29 (7) e21723 (2019). doi:10.1002/mmce.21723.
- 26) J.Kulkarni, A.G. Alharbi, A. Desai, C.-Y.-D. Sim, and A. Poddar, “Design and analysis of wideband flexible self-isolating mimo antennas for sub-6 ghz 5g and wlan smartphone terminals,” *Electronics*, 10 (23) 3031 (2021). doi:10.3390/electronics10233031.
- 27) H.V.Singh, D.V.S. Prasad, and S. Tripathi, “Compact tightly-coupled self-decoupled mimo antenna using internal hybrid tuning,” *IEEE Trans. Circuits Syst. II*, 69 (12) 4794–4798 (2022). doi:10.1109/TCSII.2022.3196791.
- 28) A.Armghan, S. Lavadiya, P. Udayaraju, M. Alsharari, K. Aliqab, and S.K. Patel, “Sickle-shaped high gain and low profile based four port mimo antenna for 5g and aeronautical mobile communication,” *Sci Rep*, 13 (1) 15700 (2023). doi:10.1038/s41598-023-42457-8.
- 29) A.Khan, Y. He, and Z.N. Chen, “A dual-band quad-port circularly polarized mimo antenna based on a modified jerusalem-cross absorber for wireless communication systems,” *IEEE Trans. Antennas Propagat.*, 72 (1) 310–322 (2024). doi:10.1109/TAP.2023.3326285.
- 30) L.Qu, “Common-loop mimo antenna design with decoupling inductors using characteristic mode analysis,” *Antennas Wirel. Propag. Lett.*, 22 (12) 3172–3176 (2023). doi:10.1109/LAWP.2023.3312690.
- 31) N.-W.Liu, B.-B. Huang, L. Zhu, and G. Fu, “Isolation and bandwidth improvements of multimode single mpa with copolarized pattern using characteristic modes analysis,” *Antennas Wirel. Propag. Lett.*, 22 (6) 1356–1360 (2023). doi:10.1109/LAWP.2023.3242087.
- 32) H.Li, W. Zheng, Q. Wu, and G.-L. Liu, “Pattern synthesis for lossy antennas based on n -port characteristic mode analysis,” *IEEE Trans. Antennas Propagat.*, 71 (6) 4628–4639 (2023). doi:10.1109/TAP.2023.3256534.

- 33) J.Kulkarni, A. Desai, and C.-Y.D. Sim, "Wideband four-port mimo antenna array with high isolation for future wireless systems," *AEU - International Journal of Electronics and Communications*, 128 153507 (2021). doi:10.1016/j.aeue.2020.153507.
- 34) I.Khan, K. Zhang, L. Ali, and Q. Wu, "Enhanced quad-port mimo antenna isolation with metamaterial superstrate," *Antennas Wirel. Propag. Lett.*, 23 (1) 439–443 (2024). doi:10.1109/LAWP.2023.3328002.
- 35) A.W.M.Saadh, P. Ramaswamy, and T. Ali, "A cpw fed two and four element antenna with reduced mutual coupling between the antenna elements for wireless applications," *Appl. Phys. A*, 127 (2) 88 (2021). doi:10.1007/s00339-020-04224-8.
- 36) P.Kumar, T. Ali, and M.P. Mm, "Characteristic mode analysis-based compact dual band-notched uwb mimo antenna loaded with neutralization line," *Micromachines*, 13 (10) 1599 (2022). doi:10.3390/mi13101599.
- 37) J.Raghunath, P. Kumar, T. Ali, P. Kumar, P. Shariff Bhadravathi Ghouse, and S. Pathan, "A quad-port nature-inspired lotus-shaped wideband terahertz antenna for wireless applications," *JSAN*, 12 (5) 69 (2023). doi:10.3390/jsan12050069.